Collecting Particulate Matter and Particle-Bound Polycyclic Aromatic Hydrocarbons Using a Cylindrical Thermal Precipitator

Shu Su[1]; Bin Wang[2]; Nan Lin[3]; Shaojie Zhuo[4]; Junfeng Liu[5]; Xilong Wang[6]; Hefa Cheng[7]; Da-Ren Chen[8]; Eddy Y. Zeng[9]; and Shu Tao[10]

Abstract: Thermophoresis has been used to develop various thermal precipitators; however, their collection performance for ambient particulate matter (PM) with an aerodynamic diameter less than 10 μm (PM_{10}) has been rarely reported, and the effect of the temperature gradient adopted in the precipitator on the evaporation loss of the organic fraction of collected particles has not been discussed to the authors' knowledge. In this study, a cylindrical thermal precipitator consisting of two coaxially aligned cylinders with an annular space of 0.51 mm and a two-inlet impactor was designed for collecting PM_{10}. The effects of the sampling flow rate and temperature gradient on the collection efficiency were examined. The precipitator was also tested for its collection efficiency for particle-bound polycyclic aromatic hydrocarbons (PAHs). At a temperature gradient of 72.6°C/mm and a flow rate of 7.74 L/min, the collection efficiency could reach 100% for PM with an electrical mobility diameter (D_p) < 0.5 μm and decreased gradually to 70% as D_p increased from 0.5 to 1.0 μm. For PM with D_p > 1.0 μm, the collection efficiency increased due to impaction at the inlet. The collection efficiency increased with an increase in the temperature gradient or a decrease in the inlet flow rate. The semiempirical model could reasonably fit the collection efficiency curve of the precipitator. No significant evaporation loss of PAHs was found when the temperature of the cold cylinder surface was approximately 0°C. It was concluded that the thermal precipitator could be used to collect ambient fine PM with a size less than 0.5 μm, and the inlet impactor design could improve the collection efficiency for coarse particles. **DOI: 10.1061/(ASCE)EE.1943-7870.0001215.**

Author keywords: Thermophoresis; Thermal precipitator; Particulate matter; Polycyclic aromatic hydrocarbon; Sampling; Collection efficiency.

Introduction

The effects of ambient particulate matter (PM) on air quality and human health have been of wide concern (Pope and Dockery 2006; Zhang and Smith 2007). These effects are believed to be related to the physical and chemical properties of PM (Hetland et al. 2004; Zhang and Smith 2007; Araujo and Nel 2009; Volckens et al. 2009; Wang et al. 2013). Traditional sampling technology for ambient PM may cause problems in recovering the original aerosol completely from the sampling substrate (Bein and Wexler 2015). Filtration is the most commonly used technique for ambient PM sampling. The PM collected on a filter can be directly quantified using a gravimetric method or quantitatively characterized for various chemical properties when it is not separated from the filter. However, for a special purpose such as in vitro toxicity tests, it is difficult to completely recover the collected PM even when using sonication extraction (Gualtieri et al. 2010). Moreover, changes in the physical properties (e.g., morphology and size distribution) of the sampled PM may occur during the extraction process (Kim et al. 2001). An alternative method for collecting ambient PM with less physical alteration is impaction. During impaction, the collected particles may aggregate in a relatively small area on the deposition substrate (Hinds 1999). Although removal of PM from an impactor by ultrasonication is easier than that from a filter, it can still affect the structure and morphology of the collected PM (Bein and Wexler 2014).

Based on the principle of thermophoresis, thermal precipitators have been developed for collecting particles (Talbot et al. 1980). A weak thermophoretic force can retain the collected particles with minimal physical alteration during their precipitation (Dobbins and Megaridis 1987). In the past, thermal precipitators of various geometric designs including hot wire, tube to tube, disk to disk, and plate to plate have been developed for various purposes (Thayer et al. 2011; Miller et al. 2012). The sampling processes of these

[1]Ph.D. Candidate, Laboratory of Earth Surface Processes, College of Urban and Environmental Sciences, Peking Univ., Beijing 100871, China.
[2]Lecturer, Institute of Reproductive and Child Health, Ministry of Health Key Laboratory of Reproductive Health, School of Public Health, Peking Univ., Beijing 100191, China.
[3]Ph.D. Candidate, Laboratory of Earth Surface Processes, College of Urban and Environmental Sciences, Peking Univ., Beijing 100871, China.
[4]Ph.D. Candidate, Laboratory of Earth Surface Processes, College of Urban and Environmental Sciences, Peking Univ., Beijing 100871, China.
[5]Associate Professor, Laboratory of Earth Surface Processes, College of Urban and Environmental Sciences, Peking Univ., Beijing 100871, China.
[6]Associate Professor, Laboratory of Earth Surface Processes, College of Urban and Environmental Sciences, Peking Univ., Beijing 100871, China.
[7]Associate Professor, Laboratory of Earth Surface Processes, College of Urban and Environmental Sciences, Peking Univ., Beijing 100871, China.
[8]Professor, Dept. of Mechanical and Nuclear Engineering, School of Engineering, Virginia Commonwealth Univ., Richmond, VA 23284.
[9]Professor, School of Environment, Jinan Univ., Guangzhou 510632, China.
[10]Professor, Laboratory of Earth Surface Processes, College of Urban and Environmental Sciences, Peking Univ., Beijing 100871, China (corresponding author). E-mail: taos@pku.edu.cn

Note. This manuscript was submitted on July 31, 2016; approved on December 2, 2016; published online on February 22, 2017. Discussion period open until July 22, 2017; separate discussions must be submitted for individual papers. This paper is part of the ***Journal of Environmental Engineering***, © ASCE, ISSN 0733-9372.

thermal precipitators have been modeled quantitatively (Tsai and Lu 1995; Azong-Wara et al. 2009; Sagot et al. 2009). Thermal precipitators have been applied to collect smoke particles (Bredl and Grieve 1951), aerobacteria (Kethley et al. 1952), soot particles (Messerer et al. 2003), and nowadays nanoparticles (Azong-Wara et al. 2013; Leith et al. 2014). For example, a plate-to-plate thermal precipitator was investigated for its collection efficiency for submicrometer (34–300 nm) soot aerosol emitted by a modern heavy-duty diesel engine (Messerer et al. 2003). Another potential application of thermal precipitators is to collect ambient PM for in vitro toxicity tests, in which unaltered PM is preferred (Broßell et al. 2013). Unfortunately, for most in vitro tests for ambient PM, samples are collected using filtration technology and recovered by ultrasonic extraction (Alfaro-Moreno et al. 2002; Hetland et al. 2004). As a result, alterations in the properties and toxicities of the collected PM are inevitable (Kim et al. 2001). Moreover, the recovery of ultrafine particles (less than 0.1 μm) from the filters is relatively low (Becker and Soukup 2003). In contrast, thermal precipitators are particularly effective for fine particles with diameters less than 0.5 μm (Wang et al. 2012a), and the sampled PM is readily rinsed off from the surface of the precipitator causing minimal changes in the PM morphology.

Although laboratory-generated particles have been widely used to test the collection performance of thermal precipitators, the collection efficiency for ambient PM with an aerodynamic diameter less than 10 μm (PM_{10}) with different morphologies and structures has not been fully studied. Because a temperature gradient has to be used in thermal precipitators, the loss of semivolatile or volatile components may occur during the sampling. To the authors' knowledge, the loss of particulate phase polycyclic aromatic hydrocarbons (PAHs) collected by the thermal precipitator due to evaporation has not been investigated. The main objectives of this study were to design a cylindrical thermal precipitator for collecting ambient PM with a large sampling flow rate and evaluate its collection performance for ambient PM_{10}. The collection efficiency for ambient PM with sizes ranging from 10 nm to 5 μm was tested. The effects of flow rates and temperature gradients on the collection efficiency were also determined. A semiempirical model was developed to quantify the sampling process. Finally, the precipitator was applied to collect particle-bound volatile or semivolatile PAHs to indicate the possible loss of organic compounds.

Methodology

Thermal Precipitator Design

Fig. 1 shows the design of the cylindrical thermal precipitator. The basic design was similar to a previous system (Wang et al. 2012b), but the following improvements were made: (1) the sampling flow rate was enlarged from 0.5–1.5 L/min to 7–12 L/min; (2) a two-path design was used for both the inlet and outlet to improve the mixing status of the inflow and outflow; and (3) a commercial aluminum pneumatic cylinder with a relatively low surface roughness ($R_a = 0.4$ μm, Yantai Hydraulic and Pneumatic Cylinder Factory, Yantai City, China) was used as the hot tube to simplify the processing technique and make the temperature field more uniform.

The hot tube was wrapped by a 300-W silicone heating plate. Cold water flowing through the cold tube was supplied by a hydrocooling water circulating pump (450 W, CCA-20, Gongyi Yuhua, Zhengzhou, Henan, China). The temperatures of the hot and cold tubes were monitored by five sensors (PT100) and controlled by a temperature controller (Jiangyin Baicheng, Wuxi, Jiangsu, China). The temperature difference between the two cold-tube sensors or among the three hot-tube sensors was less than 2 K. The relative humidity of the inflow was controlled to be below 35% using a homemade diffusion dryer. For ambient air sampling, the thermal

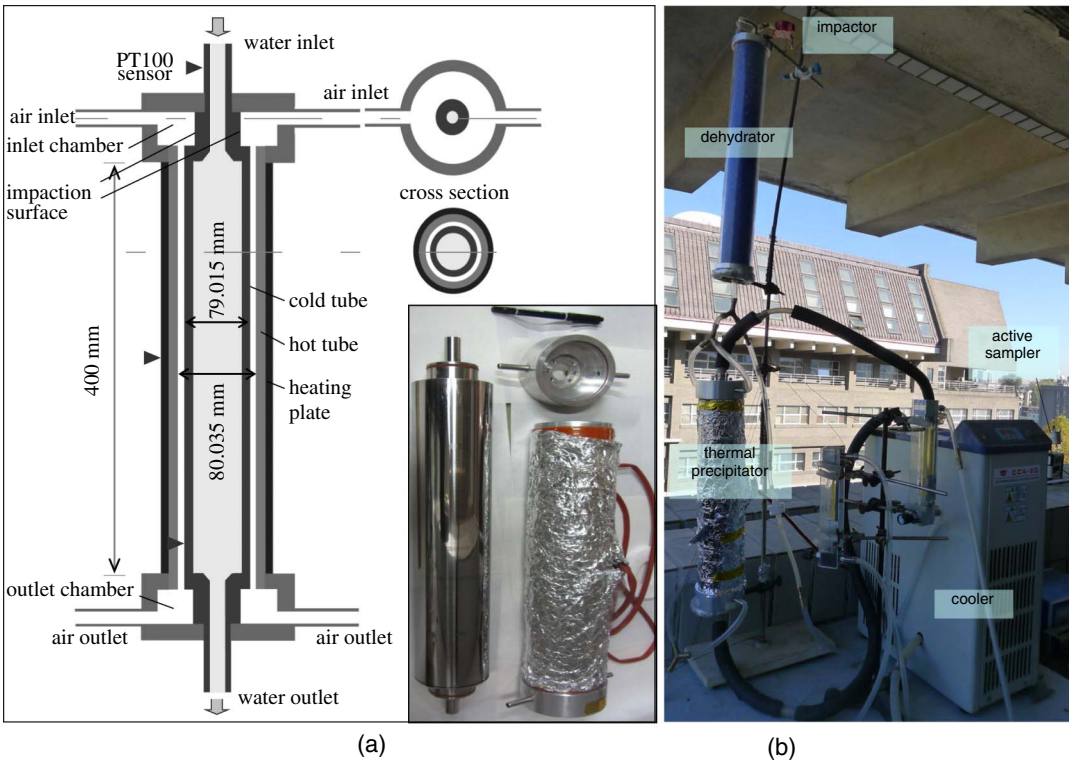

Fig. 1. (a) Design of the cylindrical thermal precipitator (a longitudinal section, a cross section, and a picture of the device); (b) deployment of the sampler in the field (with cooler, dehydrator, impactor, and active sampler) (images by Bin Wang)

J. Environ. Eng., 2017, 143(6): 04017013

precipitator was set up vertically with the aerosol inlet on the top, and the air flow rate was controlled by a valve prior to the vacuum pump (Kangjie Instrument, Liaoyang, Liaoning, China).

Modeling

The performance of the precipitator was modeled semiempirically. The collection of ambient PM by the vertically operated precipitator is mainly due to particle diffusion and thermal deposition on the cold-tube surface as well as impaction at the inlet (Marple and Willeke 1976; Hinds 1999). Based on the calculated Reynolds number (9.05) (Sagot et al. 2009) in the annular space at a flow rate of 20 L/min, a room temperature of 20°C, and the relatively short hydrodynamic entrance length (0.38 mm) (Schlichting 1979), the laminar flow and fully developed velocity profile were obtained.

For the diffusion, the following equation was adopted from Hinds (1999) and Wang et al. (2012b) to calculate the deposition efficiency (η_d):

$$\eta_{\mathrm{d}} = \frac{AU_d}{Q}, \qquad U_d = \sqrt{\frac{D}{\pi t}}, \qquad D = \frac{k_B T C_C}{3\pi\nu D_p} \tag{1}$$

where A and Q = deposition area (0.0993 m^2) and air flow rate (m^3/s), respectively; U_d = diffusion velocity (m/s); D = diffusion coefficient (m^2/s) at temperature T (average temperature of the hot and cold tubes in kelvins), t (s) = average duration for particles to reach the deposition surface; k_B = Boltzmann constant ($1.3806504 \times 10^{-23}$ J/K) (Mohr et al. 2008); ν = air kinematic viscosity (1.51×10^{-5} m^2/s) (Bird et al. 2002); D_p (m) = particle diameter; and C_c = Cunningham slip correction factor, which can be calculated as follows:

$$C_C = 1 + Kn(A + B \cdot e^{(-C \cdot Kn)}), \qquad Kn = \frac{2\lambda}{D_p} \tag{2}$$

where A (1.17), B (0.483), and C (0.997) = empirical constants from the literature (Azong-Wara et al. 2009); and Kn = ratio of the molecular mean free path length (λ, 0.066 μm at room temperature) (Bird et al. 2002) to the particle radius ($0.5D_p$).

As for impaction, the deposition efficiency is a function of the square root of the Stokes number (Stk) (Hinds 1999). The formula varies depending on the geometry and size of the impactor (Marple and Willeke 1976). For the precipitator used in this study, the semiempirical equation for calculating the deposition efficiency due to impaction (η_i) is as follows:

$$\eta_i = 2 \cdot e^{[a(\sqrt{\mathrm{Stk}} - b)]}, \qquad \mathrm{Stk} = \frac{\rho_p D_p^2 u C_c}{9\nu D_{\mathrm{nozzle}}} \tag{3}$$

where a and b = empirical coefficients that are functions of Q; ρ_p = average ambient PM density (1.73 g/cm^3) (Hu et al. 2012); u = average velocity through the inlet nozzle (sectional area is 2.83×10^{-5} m^2); and D_{nozzle} = diameter of the inlet nozzle (6.00×10^{-3} m).

In the case without a temperature gradient, the deposition of particles on the precipitator is due to impaction and diffusion, and the overall collection efficiency of the two serial processes (η_0) can be expressed as

$$\eta_0 = \eta_i + \eta_d(1 - \eta_i) \tag{4}$$

By using Eqs. (1) and (3), the measured sampling efficiencies at three flow rates of 7.74, 12.4, and 18.3 L/min without a temperature gradient were fitted to calculate the empirical constants of t, a, and b in the equations.

With the existence of a temperature gradient, a semiempirical equation was adopted for calculating a dimensionless thermophoretic velocity (U_t)

$$U_t = C \cdot e^{[-\tau/(Kn)]} \tag{5}$$

where C and τ = empirical constants, which were assigned as 0.548 and 0.0273 based on the literature (Wang et al. 2012b). The following empirical equation was used to calculate the collection efficiency due to thermophoresis (η_t):

$$\eta_t = \frac{A}{Q} \cdot \frac{\nu}{T} \cdot \frac{T_h - T_c}{R_h - R_c} \cdot U_t \tag{6}$$

where T_h and T_c = temperatures (K) of the hot and cold plates, respectively; and R_c (79.015 mm) and R_h (80.035 mm) = outer diameter of the cold tube and inner diameter of the hot tube, respectively. Eq. (3) was used to model the impaction process. Based on the measured results, the diffusion loss was insignificant, and the thermophoretic process is dominant. Therefore, the overall collection efficiency (η_{total}) can be expressed as

$$\eta_{\mathrm{total}} = \eta_i + \eta_t(1 - \eta_i) \tag{7}$$

Particulate Matter Collection Efficiency

Ambient PM collected on the roof of Yifu Building No. 2 on the campus of Peking University was used to test the performance of the precipitator. The size distribution of ambient PM_{10} was measured using a wide-range particle spectrometer (WPS, Model 1000XP, MSP, Shoreview, Minnesota) at the upstream and downstream of the precipitator alternatively to derive the size distribution of the PM collected by the precipitator. The aerosol spectrometer combines differential mobility analysis and condensation particle counting to measure particles ranging from 10 to 500 nm, and a laser particle spectrometer for particles in a range from 350 to 10,000 nm, providing a maximum of 120 particle-size channels. The count accuracy is ±10%. The instrument was calibrated immediately prior to the use. To test the influence of the sampling flow rate and temperature gradient, the measurements were performed at four temperature gradients of 0 (30.0°C for both tubes), 58.8 (42.1 and 12.1°C for the hot and cold tubes, respectively), 72.6 (49.3 and 12.2°C), and 100°C/mm (66.0 and 15.0°C) as well as three flow rates of 7.74, 12.4, and 18.3 L/min. In fact, the result of one more temperature gradient around 25°C/mm would help because the efficiencies were very different between the gradient of 0 and 58.8°C/mm, which was not recognized during the experiment design period. If a build-in temperature and flow-rate regulating device can be added in future improvement, the application of the sampler can be more flexible.

Collection Efficiency of Particle-Bound PAHs

The thermal precipitator was coupled with a quartz filter (25-mm diameter) at the outlet to evaluate the ability to collect PM for the chemical analysis of PAHs. The collection efficiency of the thermal precipitator was calculated based on the PM trapped on the precipitator and that caught by the filter. The precipitator was set at a temperature gradient of 110°C/mm (68.0 and 12.1°C for the hot and cold tubes, respectively) and a flow rate of 9.0 L/min. The 68°C was the highest temperature that can be achieved for the hot tube during the study and was chosen to see possible evaporation of PAHs. A median volume active sampler (TH-105C, Wuhan Tianhong Co., Wuhan, Hubei, China) with a quartz filter (25-mm diameter) was simultaneously operated at the same flow rate to check the overall performance. Because the breakthrough of PAHs on filters was not measured, the efficiency measured in this study is a relative term in comparison with the conventional filter sampling.

Analysis of PAHs

The extraction, cleanup, analysis, and quality control for the PAH measurement have been described previously (Shen et al. 2011). In brief, the PM collected on the cold-tube surface was washed off using ultrapure water after the cold tube was removed from the sampler, and the suspension was filtered through a 0.22-μm (37-mm) polytetrafluoroethylene (PTFE) membrane. The PTFE filter and the quartz filter were extracted with a 25-mL mixture of hexane and acetone (1:1) using a microwave-accelerated reaction system (CEM, Mars Xpress, Sausalito, California). The filtrate was extracted twice with 30 mL of *n*-hexane for 3 min each time on a shaker at 300 revolutions per minute (rpm), and the organic fraction was concentrated. A silica and alumina gel cleanup column (30 cm × 10 mm inside diameter) containing 12 cm of alumina, 12 cm of silica gel, and 1 cm of anhydrous sodium sulfate from the bottom to top and conditioned with 10 mL of *n*-hexane was used for cleanup. The column was eluted with 50 mL of *n*-hexane and dichloromethane (1:1, volume-to-volume ratio), and the eluate was concentrated to approximately 1 mL. The eluate was spiked with five mixed internal standards (naphthalene-d_8, acenaphthene-d_{10}, anthracene-d_{10}, chrysene-d_{12}, and perylene-d_{12}, J&K Chemical, Chaoyang, Beijing, China) covering a wide range of molecular weights, which are similar to those of the targeted compounds. However, the limited number of internal standards would lead to some uncertainty. Fortunately, this is a comparative study, and the effect of absolute errors is limited.

The PAH analysis was performed using a gas chromatograph-mass spectrometer (Agilent, Santa Clara, California) in the electron ionization (EI) mode with a HP-5MS capillary column. Helium was used as the carrier gas. The oven temperature was first held at 50°C for 1 min, gradually heated to 150°C at the rate of 10°C/min, then to 240°C at a slower rate of 3°C/min, and finally to 280°C in 20 min. Twenty-five parent PAHs were identified by their retention times along with the qualitative ions of the internal standards, including acenaphthene (ACE), acenaphthylene (ACY), fluorene (FLO), phenanthrene (PHE), anthracene (ANT), fluoranthene (FLA), pyrene (PYR), benz(a)anthracene (BaA), chrysene (CHR), benzo(b) fluoranthene (BbF), benzo(k)fluoranthene (BkF), benzo(a)pyrene (BaP), dibenz[a,h]anthracene (DahA), indeno(1,2,3-cd)pyrene (IcdP), benzo(g,h,i)perylene (BghiP), benzo[c]phenanthrene (BcP), retene (RET), perylene (PER), benzo(e)pyrene (BeP), coronene (COR), dibenzo[a,e]fluoranthene (DaeF), cyclopenta[c,d]pyrene (CPP), dibenzo[a,c]pyrene (DacP), dibenzo[a,l]pyrene (DalP), and dibenzo [a,e]pyrene (DaeP).

Procedural blanks were included in all experiments and subtracted from the final results. The detection limits for PAHs were 0.53–1.32 ng/g, and the recoveries of spiked standards were 77–110%. As for the surrogates, the recoveries varied from 64.9 to 116% for 2-fluoro-1,1′-biphenyl and from 94.5 to 102% for *p*-terphenyl-d_{14} (J&W Chemical, Chaoyang, Beijing, China). Triplicate samples were collected and analyzed.

Results and Discussion

Collection Efficiency with Size

The measured size distribution of ambient PM_{10} (number and volume concentrations varying with particle size) at the inlet and outlet under a temperature gradient of 72.6°C/mm and a flow rate of 12.4 L/min are shown in Fig. 2. The number concentrations were converted to volume concentrations by assuming spherical particles. The absolute difference in the PM concentration between the inlet and outlet and the collection efficiency (the concentration difference divided by the inlet concentration) are also presented. It seems that the major size distribution of PM number concentration ranges from 0.01 to 0.4 μm with a peak at approximately 0.05 μm. In terms of the volume concentration, the size of most PM varies from 0.05 to 1 μm with the main peak near 0.3 μm. The PM size distribution at the inlet and the difference between the inlet and outlet are generally similar, indicating that the distribution of ambient PM can be retained during sampling by the precipitator. The overall collection efficiency over the size range from 0.01 to 5.4 μm was 78% under a temperature gradient of 72.6°C/mm and a flow rate of 12.4 L/min. Approximately 79.8% of the collected PM (by number) was less than 0.1 μm, and the average collection efficiency was 85.4%. As D_p increased from 0.1 to 1 μm, the collection efficiency decreased to 41.0% gradually. Similar trends have been observed previously for thermal precipitators with different designs using monodisperse laboratory-generated particles (Tsai and Lu 1995; Wang et al. 2012a, b). For example, the collection efficiency for sodium chloride (NaCl) particles decreased up to 20% as the particle size increased from 0.04 to 0.5 μm (Tsai and Lu 1995; Wang et al. 2012a). As for the PM larger than 1 μm, the collection efficiency increased sharply to 90% due to the impaction and deposition of particles on the substrate (inner tube surface) at the inlet. The particle deposition at the inlet could be detected visually. The results indicated that the precipitator could trap a large fraction of fine PM, especially the ultrafine PM, and the collection efficiency for coarse PM could be significantly improved if inlet impactors were designed.

Effect of the Thermophoretic Temperature Gradient

The effect of the temperature gradient on the collection efficiency of the precipitator for ambient PM was determined by conducting

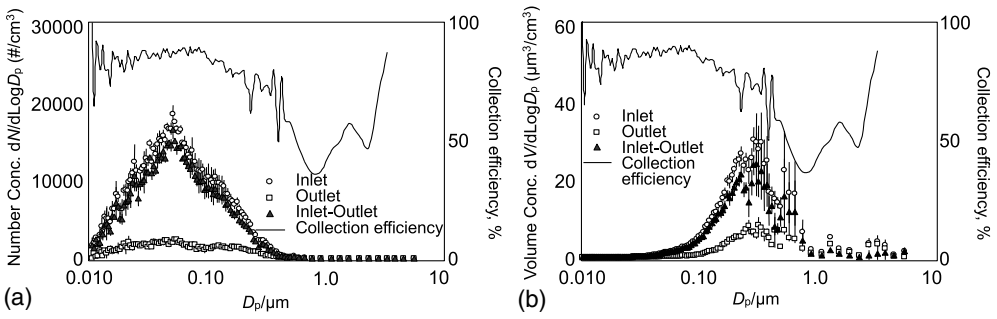

Fig. 2. Particulate matter size distribution (as electrical mobility diameter, D_p) measured at the inlet and outlet of the operating precipitator and the difference between them; the sampling efficiency was calculated by dividing the difference (inlet−outlet) by that measured at inlet; the results are shown as means and standard errors (bars) of both (a) number and (b) volume concentrations; the precipitator was operated at a 72.6°C/mm temperature gradient and a 12.4 L/min flow rate

J. Environ. Eng., 2017, 143(6): 04017013

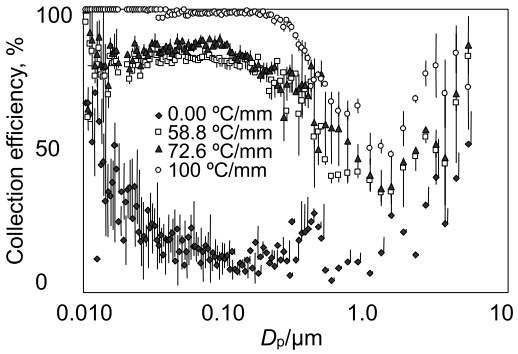

Fig. 3. Effect of temperature gradient on the sampling efficiency as percentages of PM deposited on the precipitator at a fixed flow rate of 12.4 L/min and different temperature gradients of 0, 58.8, 72.6, and 100°C/mm; the measurements are presented as means (symbols) and standard errors (bars) as functions of the electrical mobility diameter (D_p)

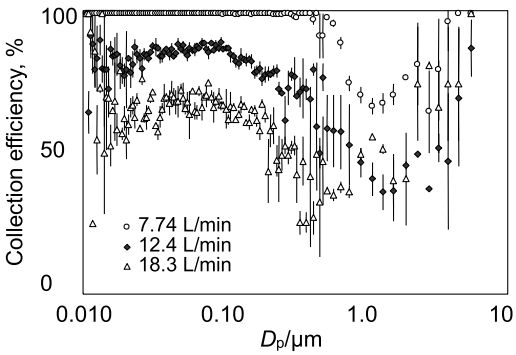

Fig. 4. Effects of flow rate on the collection efficiency at flow rates of 7.74, 12.4, and 18.3 L/min under a fixed temperature gradient of 72.6°C/mm; the measurements are presented as means (symbols) and standard errors (bars) as functions of the electrical mobility diameter (D_p)

the experiment without (0°C/mm) and with three temperature gradients of 58.8, 72.6, and 100°C/mm, respectively, as shown in Fig. 3. Overall, the collection efficiency increased as the temperature gradient increased. A higher temperature gradient can create a larger net force pushing particles to migrate along the decreasing temperature gradient (Talbot et al. 1980), thus increasing the collection efficiency. Under no temperature gradient, particles of different sizes could deposit on the precipitator, and the collection efficiency increased as the particle size decreased resulting from particle diffusion, which is a size-dependent random process with faster diffusion for finer particles (Hinds 1999). Therefore, under no temperature gradient conditions, a relatively larger fraction of fine PM (<0.04 μm) deposited on the precipitator, and the diffusion loss for larger sized PM (from 0.02 to 2 μm) was much less, which was consistent with the previous study (Tsai and Lu 1995).

At the temperature gradient of 100°C/mm and the flow rate of 12.4 L/min, the collection efficiency for particles smaller than 300 nm reached almost 100%. The efficiency decreased to 80% as the temperature gradient decreased from 100 to 72.6°C/mm, but the efficiency only decreased slightly as the gradient decreased further to 58.8°C/mm, suggesting a nonlinear dependence of the collection efficiency on the temperature gradient. The sharp increase in the diffusion rate for particles smaller than 0.2 μm was dominated by the thermophoretic process once the temperature gradient existed. The collection efficiency dropped quickly as the particle size increased from 0.3 to 2 μm at various temperature gradients, likely due to the relatively low effect of the thermophoretic force on large particles. The collection efficiency for PM with a size greater than 1 μm increased slowly, indicating the weak effect of the temperature gradient on the thermophoretic velocity of the particles. This was consistent with previous studies using artificial standard polystyrene latex particles (Wang et al. 2012b), which found that the collection efficiency induced by thermophoresis was almost zero for particles with sizes of approximately 1 μm.

Effect of the Sampling Flow Rate

The collection efficiencies at three flow rates of 7.74, 12.4, and 18.3 L/min under a fixed temperature gradient of 72.6°C/mm are shown in Fig. 4. At the lowest flow rate of 7.74 L/min, the collection efficiency for PM with D_p less than 0.5 μm was nearly 100%. The collection efficiency decreased sharply for PM larger than 0.5 μm. When the flow rate increased, the collection efficiency decreased significantly, especially for PM larger than 0.2 μm.

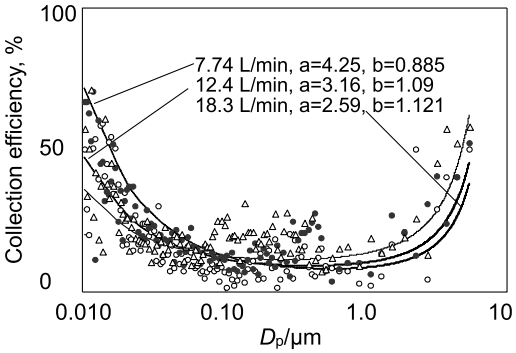

Fig. 5. Fitting the measured PM sampling efficiencies of the precipitator at three flow rates of 7.74 (hollow triangles), 12.4 (solid circles), and 18.3 (hollow circles) L/min without temperature gradient; the measured data are shown as symbols; the modeled curves were derived from least-squares fitting

For ultrafine PM, the collection efficiency dropped from 100 to 80–85% as the flow rate increased from 7.74 to 12.4 L/min, and it dropped to 60–65% as the flow rate reached 18.3 L/min. Due to the impaction at the inlet, the PM collection efficiency increased as D_p increased from 1 to 5 μm at all three flow rates. These results suggested that the larger the flow rate, the lower the collection efficiency at a relatively high temperature gradient.

Modeling Results

The measured results could be described by Eq. (4), and the fitted curves at the three flow rates under no temperature gradient are shown in Fig. 5. The constant t is 0.0252 s for all flow rates. The calculated a values are 4.25, 3.16, and 2.59, and the b values are 0.885, 1.09, and 1.21 for the three flow rates, respectively. According to Eq. (7), the measured sampling efficiencies at the three flow rates of 7.74, 12.4, and 18.3 L/min with a temperature gradient of 38.2°C/mm were fitted using the least-squares method. With a temperature gradient applied, the impaction could also be affected and was modeled together with the thermophoretic process. The results are shown in Fig. 6 as three curves. The calculated a values are 3.67, 2.73, and 2.24, and the b values are 0.765, 0.944, and 1.05 for the three flow rates, respectively. Overall, the fitting curves could be reasonably in agreement with the experimental results. However, the modeling may be affected by the uncertainty of points

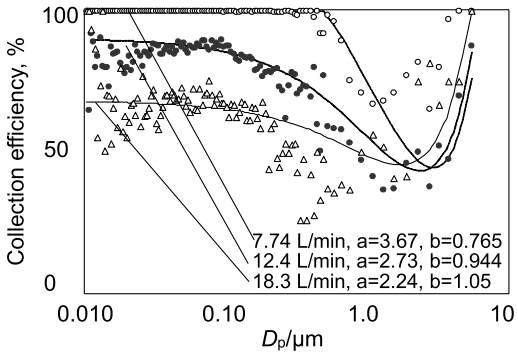

Fig. 6. Fitting the measured PM sampling efficiencies of the precipitator at three flow rates of 7.74 (hollow circles), 12.4 (solid circles), and 18.3 (hollow triangles) L/min with a temperature gradient of 38.2°C/mm; the measured data are shown as symbols; the modeled curves were derived from least-squares fitting

above 1 μm due to their low collection efficiency (under 41%). The semiempirical modeling formula can provide a general design idea for a thermal precipitator to collect ambient particles.

Collection of Particle-Bound PAHs

To evaluate the collection efficiency of the thermal precipitator for particle-bound PAHs, the precipitator coupled with a quartz filter (F_p) at the outlet was tested. Samples collected by the precipitator included those deposited on the cold tube by thermal precipitation (P_{th}) and those caught by impaction at the inlet (P_{imp}). An active sampler with a quartz filter (F_t) was also simultaneously operated at the same flow rate of 8.3 L/min. The total quantities of 25 particulate PAHs collected by the precipitator and the coupled filter were compared with those collected by the active sampler alone by calculating ratios of $(P_{\text{th}} + P_{\text{imp}} + F_p)/F_t$ to check the possible loss due to evaporation or contamination [Fig. 7(a)]. For all measured PAHs, the ratios varied but were approximately 1, indicating no significant loss or contamination during the sampling. Thus, the temperature gradient in the thermal precipitator did not increase the evaporation of volatile or semivolatile compounds, mainly because the sampling particles were deposited on the cold surface of the precipitator in several seconds and this could not cause the evaporation of PAHs. Blow-off losses of PAHs from the collected particles cannot be avoided for both the filter and precipitator. Taking into consideration the difference in the flow passing the surface of the collected particulates between the two sampling methods, the loss is expected to be relatively small for the precipitator.

The relative contents of the 25 PAH compounds collected by P_{imp}, P_{th}, and F_p are shown in Fig. 7(b). On average, only 4.47% of PAH compounds passed through the thermal precipitator (F_p). The overall recovery varied from 91.5 (DalP) to 100% (DaeP). Thermal precipitation represented 94.1% of the total collected PAHs, with the exceptions of the four low-ring PAHs with smaller molecular weights, including ACE, FLO, PHE, and ANT. It has been reported that high-ring PAHs tend to be present in fine particles, while for low-ring PAHs, such a preference is not observed (Wang et al. 2013). Based on the previous discussion, coarse PM was mainly collected at the inlet due to impaction, and fine PM was collected by the precipitator. Therefore, the particle-bound high-ring PAHs were collected more efficiently than the low-ring PAHs in the precipitator.

Conclusion

The collection efficiency of the precipitator is positively correlated with the temperature gradient and negatively correlated with the inlet flow rate (at a relatively high temperature gradient). The precipitator is particularly effective for the collection of ambient fine particles. The collection efficiency could reach approximately 100% for PM with an electrical mobility diameter (D_p) smaller than 0.5 μm by adjusting the sampling flow rate and thermophoretic temperature gradient. The collection efficiency for coarse PM can be significantly improved by the inlet impactor. The proposed semiempirical model could provide a general idea for designing a thermal precipitator for collecting ambient PM. The temperature gradient in the precipitator did not increase the evaporation loss of PAHs, and the collection efficiency was higher for high-ring PAHs.

Acknowledgments

Funding for this study was provided by the National Natural Science Foundation of China (41390240, 41571130010, and 41130754). The authors express their great appreciation to Dr. Arantzazu Eiguren-Fernandez and Dr. Raymond Coveney for their help in editing this article.

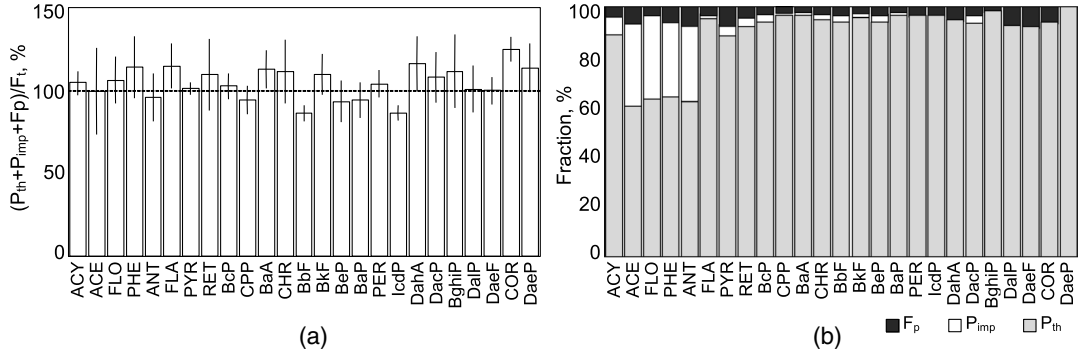

Fig. 7. Recoveries of individual PAH compounds by the thermal precipitator operated at a 105°C/mm temperature gradient (52 and −1.6°C for hot and cold tubes, respectively) and a 8.3 L/min flow rate: (a) ratios (means and standard errors) of the total quantity collected by the precipitator ($P_{\text{th}} + P_{\text{imp}}$) coupled with a filter after precipitator (F_p) to that collected by an active sampler with filter alone (F_t); (b) fractions of individual PAH compounds collected by the thermal precipitation (P_{th}), impaction (P_{imp}), and the filter (F_p) of the coupled precipitator-filter sampling

References

Alfaro-Moreno, E., et al. (2002). "Biologic effects induced in vitro by PM_{10} from three different zones of Mexico City." *Environ. Health Persp.*, 110(7), 715–720.

Araujo, J. A., and Nel, A. E. (2009). "Particulate matter and atherosclerosis: Role of particle size, composition and oxidative stress." *Part. Fibre Toxicol.*, 6(1), 24.

Azong-Wara, N., et al. (2009). "Optimisation of a thermophoretic personal sampler for nanoparticle exposure studies." *J. Nanopart. Res.*, 11(7), 1611–1624.

Azong-Wara, N., et al. (2013). "Design and experimental evaluation of a new nanoparticle thermophoretic personal sampler." *J. Nanopart. Res.*, 15(4), 1–12.

Becker, S., and Soukup, J. M. (2003). "Coarse ($PM_{2.5-10}$), fine ($PM_{2.5}$), and ultrafine air pollution particles induce/increase immune costimulatory receptors on human blood-derived monocytes but not on alveolar macrophages." *J. Toxicol. Environ. Health A*, 66(9), 847–859.

Bein, K. J., and Wexler, A. S. (2014). "A high-efficiency, low-bias method for extracting particulate matter from filter and impactor substrates." *Atmos. Environ.*, 90, 87–95.

Bein, K. J., and Wexler, A. S. (2015). "Compositional variance in extracted particulate matter using different filter extraction techniques." *Atmos. Environ.*, 107, 24–34.

Bird, R. B., Stewart, W. E., and Lightfoot, E. N. (2002). *Transport phenomena*, 2nd Ed., Wiley, New York.

Bredl, J., and Grieve, T. W. (1951). "A thermal precipitator for the gravimetric estimation of solid particles in flue gases." *J. Sci. Instrum.*, 28(1), 21–23.

Broßell, D., et al. (2013). "A thermal precipitator for the deposition of airborne nanoparticles onto living cells—Rationale and development." *J. Aerosol Sci.*, 63, 75–86.

Dobbins, R. A., and Megaridis, C. M. (1987). "Morphology of flame-generated soot as determined by thermophoretic sampling." *Langmuir*, 3(2), 254–259.

Gualtieri, M., et al. (2010). "Differences in cytotoxicity versus pro-inflammatory potency of different PM fractions in human epithelial lung cells." *Toxicol. in Vitro*, 24(1), 29–39.

Hetland, R. B., et al. (2004). "Release of inflammatory cytokines, cell toxicity and apoptosis in epithelial lung cells after exposure to ambient air particles of different size fractions." *Toxicol. in Vitro*, 18(2), 203–212.

Hinds, W. C. (1999). *Aerosol technology: properties, behavior, and measurement of airborne particles*, 2nd Ed., Wiley-Interscience, New York, 133–148.

Hu, M., et al. (2012). "Estimation of size-resolved ambient particle density based on the measurement of aerosol number, mass, and chemical size distributions in the winter in Beijing." *Environ. Sci. Technol.*, 46(18), 9941–9947.

Kethley, T. W., Gordon, M. T., and Orr, C., Jr. (1952). "A thermal precipitator for aerobacteriology." *Science*, 116(3014), 368–369.

Kim, S., Jaques, P. A., Chang, M. C., Froines, J. R., and Sioutas, C. (2001). "Versatile aerosol concentration enrichment system (VACES) for simultaneous in vivo and in vitro evaluation of toxic effects of ultrafine, fine and coarse ambient particles—Part I: Development and laboratory characterization." *J. Aerosol Sci.*, 32(11), 1281–1297.

Leith, D., Miller-Lionberg, D., Casuccio, G., Lersch, T., Lentz, H., Marchese, A., and Volckens, J. (2014). "Development of a transfer function for a personal, thermophoretic nanoparticle sampler." *Aerosol Sci. Technol.*, 48(1), 81–89.

Marple, V. A., and Willeke, K. (1976). "Impactor design." *Atmos. Environ.*, 10(10), 891–896.

Messerer, A., Niessner, R., and Pöschl, U. (2003). "Thermophoretic deposition of soot aerosol particles under experimental conditions relevant for modem diesel engine exhaust gas systems." *J. Aerosol Sci.*, 34(8), 1009–1021.

Miller, A., Marinos, A., Wendel, C., King, G., and Bugarski, A. (2012). "Design optimization of a portable thermophoretic precipitator nanoparticle sampler." *Aerosol Sci. Technol.*, 46(8), 897–904.

Mohr, P. J., Taylor, B. N., and Newell, D. B. (2008). "CODATA recommended values of the fundamental physical constants: 2006." *J. Phys. Chem. Ref. Data*, 37(3), 1187–1284.

Pope, C. A., III., and Dockery, D. W. (2006). "Health effects of fine particulate air pollution: lines that connect." *J. Air Waste Manage.*, 56(6), 709–742.

Sagot, B., Antonini, G., and Buron, F. (2009). "Annular flow configuration with high deposition efficiency for the experimental determination of thermophoretic diffusion coefficients." *J. Aerosol Sci.*, 40(12), 1030–1049.

Schlichting, H. (1979). *Boundary-layer theory*, 7th Ed., McGraw-Hill, New York.

Shen, G. F., et al. (2011). "Emissions of PAHs from indoor crop residue burning in a typical rural stove: Emission factors, size distributions, and gas-particle partitioning." *Environ. Sci. Technol.*, 45(4), 1206–1212.

Talbot, L., Cheng, R. K., Schefer, R. W., and Willis, D. R. (1980). "Thermophoresis of particles in a heated boundary-layer." *J. Fluid Mech.*, 101(04), 737–758.

Thayer, D., Koehler, K. A., Marchese, A., and Volckens, J. (2011). "A personal, thermophoretic sampler for airborne nanoparticles." *Aerosol Sci. Technol.*, 45(6), 744–750.

Tsai, C. J., and Lu, H. C. (1995). "Design and evaluation of a plate-to-plate thermophoretic precipitator." *Aerosol Sci. Technol.*, 22(2), 172–180.

Volckens, J., Dailey, L., Walters, G., and Devlin, R. B. (2009). "Direct particle-to-cell deposition of coarse ambient particulate matter increases the production of inflammatory mediators from cultured human airway epithelial cells." *Environ. Sci. Technol.*, 43(12), 4595–4599.

Wang, B., et al. (2013). "Properties and inflammatory effects of various size fractions of ambient particulate matter from Beijing on A549 and J774A.1 cells." *Environ. Sci. Technol.*, 47(18), 10583–10590.

Wang, B., Ou, Q. S., Tao, S., and Chen, D. R. (2012a). "Performance study of a disk-to-disk thermal precipitator." *J. Aerosol Sci.*, 52, 45–56.

Wang, B., Tao, S., and Chen, D. R. (2012b). "A cylindrical thermal precipitator with a particle size-selective inlet." *Aerosol Sci. Technol.*, 46(11), 1227–1238.

Zhang, J. J., and Smith, K. R. (2007). "Household air pollution from coal and biomass fuels in China: measurements, health impacts, and interventions." *Environ. Health Persp.*, 115(6), 848–855.